

# Performance of human body communication-based wearable ECG with capacitive coupling electrodes

Jun Sakuma, Daisuke Anzai, Jianqing Wang ✉

Department of Computer Science and Engineering, Graduate School of Engineering, Nagoya Institute of Technology, Nagoya 466-8555, Japan

✉ E-mail: wang@nitech.ac.jp

Published in Healthcare Technology Letters; Received on 12th April 2016; Revised on 9th June 2016; Accepted on 13th June 2016

Wearable electrocardiogram (ECG) is attracting much attention in daily healthcare applications, and human body communication (HBC) technology provides an evident advantage in making the sensing electrodes of ECG also working for transmission through the human body. In view of actual usage in daily life, however, non-contact electrodes to the human body are desirable. In this Letter, the authors discussed the ECG circuit structure in the HBC-based wearable ECG for removing the common mode noise when employing non-contact capacitive coupling electrodes. Through the comparison of experimental results, they have shown that the authors' proposed circuit structure with the third electrode directly connected to signal ground can provide an effect on common mode noise reduction similar to the usual drive-right-leg circuit, and a sufficiently good acquisition performance of ECG signals.

**1. Introduction:** In the coming aging society, it is desirable to automatically collect various vital data such as blood pressure, body temperature, electrocardiogram (ECG), electroencephalogram (EEG) and so on, in daily life. The vital sensors need to have a communication function to automatically send the acquired vital data to a coordinator on the human body for forming a wireless body area network (BAN), and the coordinator then forwards the collected vital data to a hospital or medical centre for healthcare administration [1–3]. In place of usual Bluetooth technology for on-body transmission, we have previously developed a wearable ECG which employs human body communication (HBC) technology as the communication tool [4]. An evident advantage of HBC technology is that the sensing electrodes of ECG also work for transmission through the human body. The realisation of the common use of sensing and transmitting electrodes is based on a time sharing scheme, and can largely simplify the wearable ECG structure.

However, these electrodes are usually directly contacted with the human body for both sensing and transmission. Such a direct contact may cause an allergic reaction of skin, and the long-term contact may also yield a degradation of sensing/transmitting quality of electrodes. From the point of view of everyday use, non-contact electrodes are ideal. This means a capacitive coupling between the metal electrodes and the human body. A prototype system was introduced in [5] to measure impedance over capacitive electrodes, which contributed to draw a conclusion about the applicability of such capacitive electrodes for ECG detection. For realising the non-contact capacitive coupling detection, placing small flexible electrodes into cotton pockets of a worn tight NIKE Pro combat T-shirt was proposed in [6], and inserting a thin cloth between the sensing electrodes and the skin of a subject's dorsal surface was proposed in [7]. Both the two studies focus on the use of capacitive electrodes, and the detected ECG signals were confirmed useful for non-diagnostic purposes.

The capacitive coupling is easier to be affected by common mode noise produced by environmental electromagnetic field, because of the increased impedance between the electrodes and the human body. In the direct contact electrode cases, a drive-right-leg (DRL) circuit is usually used to reduce the contact resistance and then the common mode noise through a negative feedback loop, where the resistance is reduced by the open-loop gain of operational amplifier [8]. Its effect under the non-contact electrode condition,

however, is unclear. If we remove the DRL circuit, the circuit ground of differential amplifier will be connected to the human body through the third electrode which forms a capacitive coupling between the circuit ground and the human body. Such a structure can simplify the ECG detector structure, but a degradation on the suppression effect of common mode noise is worried about.

In this Letter, we aim to employ the non-contact capacitive coupling electrodes in our HBC-based wearable ECG. First, we clarify the effect of DRL circuit in the non-contact electrode case. Second we make an effort to reduce the impedances between the non-contact electrodes and the human body, and show the feasibility of just using the third electrode of ground in reducing the common mode noise. Finally, with the proposed structure of non-contact electrodes and ECG detector circuit, without the usual DRL, in the HBC-based wearable ECG, we experimentally compare the ECG acquisition performances with a commercially available ECG, and show the effectiveness of the proposed structure for getting a sufficiently good acquisition performance even in the non-contact capacitive coupling case.

**2. Structure and analysis of ECG detector:** Our developed wearable ECG consists of an ECG detector, an analogue-to-digital (AD) converter, and an HBC transceiver. The ECG detector has a differential input and is connected to two sensing electrodes and one ground electrode. The acquired ECG signal is AD-converted and send to the HBC transceiver. The HBC transceiver employs an impulse radio (IR) modulation scheme with on-off keying (OOK) and uses the two sensing electrodes also for data transmission through the human body. The electrodes for both vital signal sensing and HBC data transmission are made of two 3 × 3 cm metal plates. Table 1 summarises the specifications of the wearable ECG, and Fig. 1 shows the block diagram of the ECG detector circuit. Both the sensing electrodes and the ground electrode are non-contact with the human body. It is actually a capacitive coupling between the electrodes and skin with the cloth or air as the medium. The low-pass filters (LPFs) are used to remove high frequency interferences especially from the HBC signals and the high-pass filters (HPFs) are used to remove direct-current and drift noise components. As can be seen from Fig. 1, we can choose either the DRL circuit or the third electrode directly connected to the signal ground in the ECG detector circuit for comparison.

**Table 1** Specifications of the wearable ECG

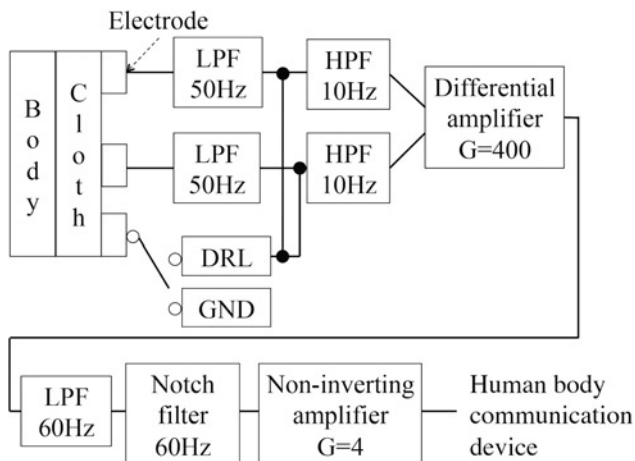
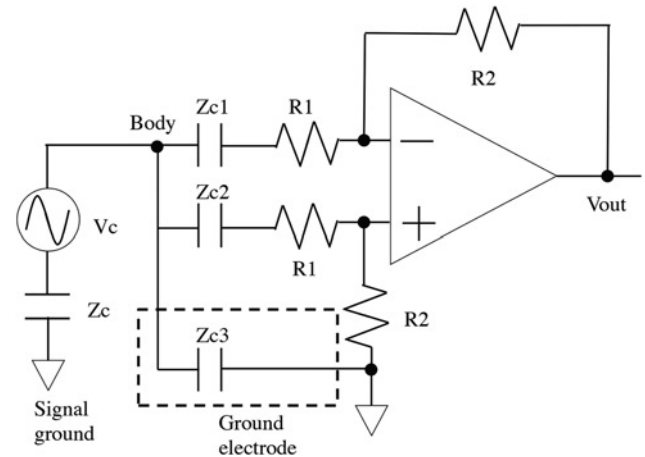
LPF cutoff frequency of ECG detector	50 Hz
HPF cutoff frequency of ECG detector	10 Hz
notch filter of ECG detector	50 or 60 Hz
amplifier gain of ECG detector	64 dB
sampling rate of AD converter	500 Hz
quantisation level of AD converter	10 bits
frequency band of HBC	10–60 MHz
data rate of HBC	1.25 Mbps
modulation scheme of HBC	IR with OOK
consumption power	4.8 mW

As described in [8], the DRL circuit usually reduces the common mode voltage by using a negative feedback loop where an additional amplifier is used to amplify and reinject the common mode noise through the third electrode. The common mode noise is the voltage between the human body and the earth ground where the human stands, and the open-loop gain of the additional amplifier contributes to reduce the impedance between the electrode and the human body. If we omit the DRL circuit, one side of the third electrode will be directly connected to the signal ground, and the other side will be connected to the human body through a capacitive coupling. Without losing generality, we can simplify the ECG detector structure into Fig. 2, where  $V_c$  is the common mode noise voltage produced by the environmental electromagnetic field, and  $Z_c = 1/j2\pi fC$  is the capacitive impedance between the signal ground of ECG detector and the earth ground where the human body stands. Since we are considering the non-contact electrode case,  $Z_{c1}$ ,  $Z_{c2}$  and  $Z_{c3}$  in Fig. 2 are capacitive impedances. These impedances are usually imbalanced due to their different attachment conditions, and as a result the common mode voltage  $V_c$  will be transferred into a differential mode interference voltage  $V_{out}$ .

From Fig. 2, under the assumption of ideal operational amplifier, the interference voltage  $V_{out}$  can be expressed as

$$V_{out} = \frac{R_2(Z_{c1} - Z_{c2})}{Z_c(Z_{c1} + Z_{c2} + 2R_1) + (Z_{c1} + R_1)(Z_{c2} + R_1 + R_2)(1 + Z_c/Z_{c3})} V_c \quad (1)$$

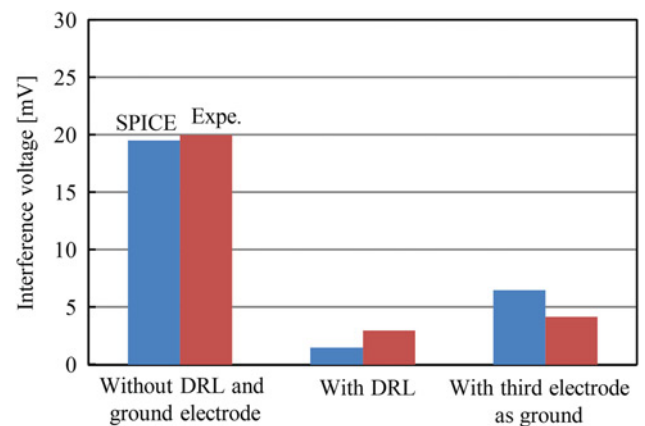
where  $Z_c/Z_{c3}$  in (1) is actually equal to  $C_3/C$ , and  $C_3$  is the capacitance between the third electrode of ground and the human body. So, different from usual contact electrode case,  $Z_c/Z_{c3} = C_3/C$  is independent from the frequency  $f$  of common mode noise. If without the third electrode of ground,  $C_3$  approaches zero, so that the interference voltage  $V_{out}$  has the largest level. While if we have a good ground electrode, i.e.  $C_3$  approaches infinity, the interference

**Fig. 1** Block diagram of ECG detector circuit**Fig. 2** ECG detector circuit with the third electrode as ground

voltage  $V_{out}$  will be removed. A large capacitance  $C_3$  (or a small impedance  $Z_{c3}$ ) is therefore effective in reducing the common mode noise.

To increase the magnitude of  $C_3$ , one method is to enlarge the area of electrodes, and another method is to employ high permittivity material as an intermediate medium. In this Letter, we investigated three types of cloth material, the cotton, polyester, and the linen, as the medium between the electrode and the skin, and found that the linen cloth exhibited the best acquisition performance because it had the highest relative permittivity (nearly 10). On the other hand, the stray impedance  $C$  is known in the order of 200 pF [9]. The ratio of  $Z_c/Z_{c3}$  or  $C_3/C$  is therefore almost constant at any frequency of common mode noise. This feature is specific in the non-contact electrode case, and contributes to provide the same reduction effect of common mode noise at all frequencies.

**3. Validation:** We then examined whether or not the use of the third electrode of ground can achieve a similar common mode reduction effect as the usual DRL circuit in the case of non-contact capacitive coupling electrodes. For the circuit shown in Fig. 2, we conducted the circuit simulation with SPICE (Simulation Program with Integrated Circuit Emphasis) and experiment for a common mode noise at 60 Hz. The operational amplifiers (Texas Instruments, TL074ACN) with an input impedance as high as 1 TΩ were employed in the experiment, because an ideal operational amplifier should have an infinitely large input impedance. Fig. 3 compares the reduced quantities of common mode noise at 60 Hz for a fixed input voltage  $V_c$ . As can be seen, the SPICE simulation and experiment gave the

**Fig. 3** Comparison of noise reduction effect

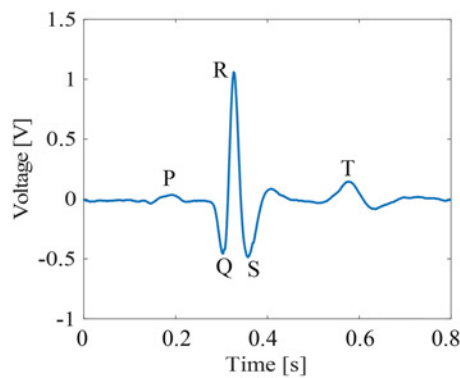


**Fig. 4** Example of amplified ECG signal waveform

similar results. With respect to the case without DRL and ground electrode, the common mode noise was decreased to 21% when using the third electrode of ground, and 15% when using the DRL. Although the DRL exhibited a better performance of noise reduction, connecting the third electrode directly to the signal ground can also reduce the common mode noise to a sufficiently small level.

**4. Performance comparison with commercial ECG:** Fig. 4 shows an example of ECG waveform measured by our HBC-based wearable ECG. Although the cutoff frequency of 10 Hz in the HPF design of Fig. 1 may be somewhat higher, it is still possible to observe not only the QRS-wave, but also the P-wave and T-wave. The QRS-wave duration was measured as 0.1 s, and the P-wave duration was measured as 0.07 s. Both of them fell in the typical range of QRS-wave and P-wave durations, i.e. 0.06–0.10 s, which supports the soundness of our HBC-based wearable ECG.

To further verify the reliability of the HBC-based wearable ECG with the third electrode of ground, but DRL removed, we compared the acquired heart rate variability in performance with a commercially available radio-frequency (RF) ECG [10]. The heart rate variability is a physiological phenomenon of variation in the time interval between heartbeats. It is measured by the variation in the beat-to-beat interval. In the time domain, the representative parameters are RR interval (RRI), RR50 and the standard deviation of RRI. While in the frequency domain, the representative parameters are low frequency (LF) heart rate fluctuation, high frequency (HF) heart rate fluctuation and LF/HF ratio.

The RF-ECG employs a narrow band modulation scheme at 2.4 GHz for transmitting ECG data. We set both our HBC-based

**Table 2** Correlation coefficient of RRI between HBC-ECG and RF-ECG

Subject	A	B	C	D	Average
	0.95	0.88	0.85	0.94	0.91

wearable ECG and the RF-ECG on the chest with an adequate spacing, and in both cases the receivers were connected to a personal computer via USB interface. It should be emphasised that the electrodes were directly contacted with the human body in the RF-ECG case, but were non-contacted with or capacitively coupled to the human body in the HBC-based ECG case. The ECG acquisition and transmission were conducted for four subjects. Fig. 5 shows the HBC-ECG-acquired RRI versus RF-ECG-acquired RRI. Tables 2 and 3 give the correlation coefficients and SDNNs between them, respectively, for the four subjects. The correlation coefficients are larger than 0.85, and the relative differences of SDNN are within 5.4%. Moreover, we also compared RR50, the ratio of the number of adjacent intervals differing by over 50 ms duration in Table 4. The symbol ‘—’ in the table means too little number of samples to calculate the relative difference. The results show that the relative differences between HBC-ECG and RF-ECG are within 8%. These results demonstrate that the HBC-based ECG provides the almost equal performance as the commercially available RF-ECG, even if we employ non-contact capacitive coupling electrodes and remove the DRL circuit.

**Table 3** Comparison of SDNN (ms) between HBC-ECG and RF-ECG

Subject	A	B	C	D	Average
HBC-ECG	29.9	80.9	27.8	46.8	46.4
RF-ECG	30.4	81.3	28.3	49.5	47.4
relative diff., %	1.7	0.5	1.8	5.4	2.4

**Table 4** Comparison of RR50 [sample] within 5 min between HBC-ECG and RF-ECG

Subject	A	B	C	D	Average
HBC-ECG	5	111	4	109	57
RF-ECG	4	103	3	102	53
relative diff., %	—	7.8	—	6.9	7.4

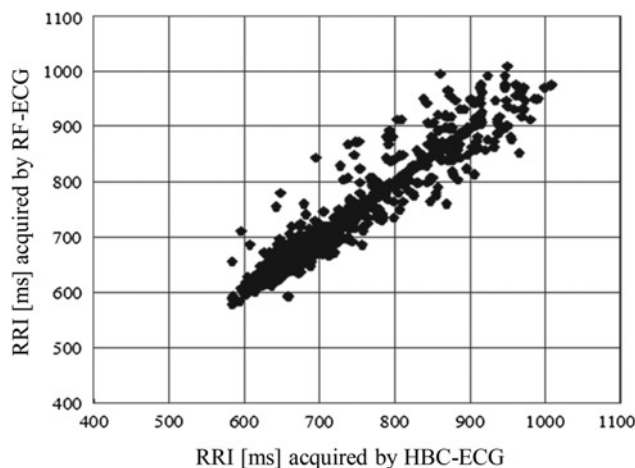


**Fig. 5** HBC-ECG-acquired RRI against RF-ECG-acquired RRI

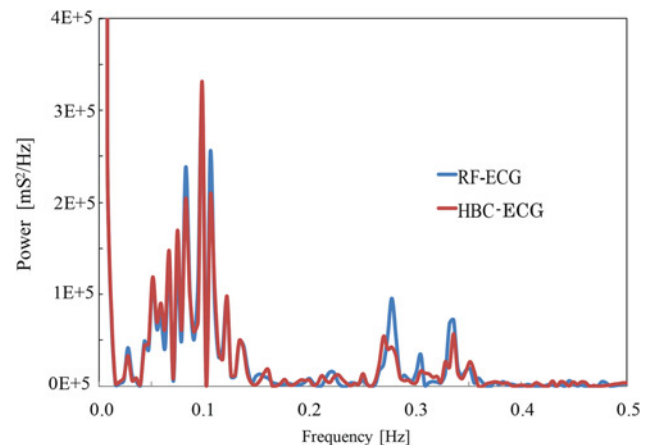


**Fig. 6** Comparison of RRI power spectra between HBC-based ECG and RF-ECG

**Table 5** Comparison of LF/HF between HBC-ECG and RF-ECG

Subject	A	B	C	D	Average
HBC-ECG	3.05	0.73	3.09	0.17	1.76
RF-ECG	3.43	0.66	2.85	0.20	1.79
relative diff., %	12.6	9.2	7.8	16.6	11.5

In addition, we also obtained the power spectrum of RRI data with Fourier transform. Fig. 6 shows the RRI power spectra for both HBC-based ECG and RF-ECG. They exhibit fair agreement at both LF range (from 0.05 to 0.15 Hz) and HF ranges (from 0.15 to 0.4 Hz). Table 5 compares the LF/HF of the integration values of power spectra between LF range and HF range. The relative differences do not exceed 16.6%. So the HBC-based ECG with non-contact capacitive coupling electrodes can provide a sufficient reliability in both the time and frequency domains. Moreover, compared to the performances shown in [6, 7], our HBC-based ECG provides a clearer QRS-wave and a clearer heart rate variability analysis result, which suggests a possibility for diagnostic purpose. As for the difference in Fig. 6, it may be due to the different measurement positions for HBC-ECG and RF-ECG on the chest, although they were set as close as possible. Another possible reason is the difference between the non-contacting capacitive electrodes in our HBC-ECG and the direct contacting electrodes in the RF-ECG. The capacitive electrodes should be more sensitive to the influence of motion artefact and common mode noise. The motion artefact may be reduced by a wavelet transform based algorithm as a software solution as introduced in [11]. While for the common mode noise, since it is added to the ECG signal by mode change due to an imbalance of impedance between sensing electrodes, our proposed imbalance cancellation circuit in [12] is effective as a hardware solution to suppress it.

**5. Conclusions:** In this Letter, we have introduced the non-contact capacitive coupling electrodes into our previously developed HBC-based wearable ECG. The non-contacting of electrodes to the human skin can provide more conveniences in the daily use of wearable vital sensors. By connecting the third electrode directly to the signal ground, we have omitted the DRL circuit usually used for common mode noise reduction, and derived a theoretical expression for the noise reduction effect of such a ground electrode. With the linen cloth to increase the capacitance between the electrodes and human body and then reduce the magnitude of impedance, we have demonstrated that the third electrode of ground can give a similar reduction effect of common mode noise as the DRL circuit, and contribute to simplify the wearable ECG structure. With this ECG detector

structure without DRL circuit, we have compared the heart rate variability performances acquired by our HBC-based wearable ECG with a commercially available RF-ECG. The comparison results for various ECG parameters in the time and frequency domains have shown good agreement and accuracy. The agreement and accuracy support the feasibility to employ capacitive coupling electrodes for both signal sensing and transmission in the HBC-based ECG, even without the DRL circuit.

In view of that the motion artefact may significantly affect the ECG detection performance, we have assumed the electrodes fixed by a belt or being a part of cloth in our wearable ECG. At the same time, we are applying a Wavelet transformation-based algorithm to reduce the motion artefact. This approach appears promising, and the result will be reported in the near future.

**6. Funding and declaration of interests:** This work was supported in part by JSPS Grants-in-Aid for Scientific Research Grant Number 15H04006. Conflict of interest: None declared.

## 7. References

- [1] IEEE Std 802.15.6-2012: IEEE Standard for local and metropolitan area networks – Part 15.6: Wireless Body Area Networks, 2012
- [2] Wang J., Wang Q.: 'Body area communications' (Wiley-IEEE, 2012)
- [3] Bonato P.: 'Wearable sensors and systems - From enabling technology to clinical applications', *IEEE Eng. Med. Biol. Mag.*, 2010, **29**, (3), pp. 25–36
- [4] Wang J., Fujiwara T., Kato T., *ET AL.*: 'Wearable ECG based on impulse radio type human body communication', *IEEE Trans. Biomed. Eng.*, 2015, doi: 10.1109/TBME.2015.2504998
- [5] Eilebrecht B., Willkomm J., Pohl A., *ET AL.*: 'Impedance measurement system for determination of capacitive electrode coupling', *IEEE Trans. Biomed. Circuits Syst.*, 2013, **7**, (5), pp. 682–689
- [6] Mathias D.N., Kim S.-I., Park J.-S., *ET AL.*: 'Real time ECG monitoring through a wearable smart T-shirt', *IEEE Trans. Electric. Electron. Mater.*, 2015, **16**, (1), pp. 16–19
- [7] Ueno A., Akabane Y., Kato T., *ET AL.*: 'Capacitive sensing of electrocardiographic potential through cloth from the dorsal surface of the body in a supine position: a preliminary study', *IEEE Trans. Biomed. Eng.*, 2007, **54**, (4), pp. 759–766
- [8] Spinelli E.M., Martinez N.H., Mayosky M.A.: 'A transconductance driven-right-leg circuit', *IEEE Trans. Biomed. Eng.*, 1999, **46**, (12), pp. 1466–1470
- [9] Liao W., Shi J., Wang J.: 'An approach to evaluate electromagnetic interference with wearable ECG at frequencies below 1 MHz', *IEICE Trans. Commun.*, 2015, **E98-B**, (8), pp. 1606–1613
- [10] [http://www.mmdevice.co.jp/english/goods\\_01.html](http://www.mmdevice.co.jp/english/goods_01.html)
- [11] Strasser F., Muma M., Zoubir A.M.: 'Motion artifact removal in ECG signals using multi-resolution thresholding'. 20th European Signal Processing Conf. (EUSIPCO), Bucharest, Romania, 2012, pp. 899–903
- [12] Noro M., Anzai D., Wang J.: 'Proposal and performance evaluation of common-mode noise cancel circuit for wearable ECG'. IEE Japan Technical Meeting on EMC, 2015, vol. **EMC-15-053**, pp. 1–4